



PolArStat: An Arduino based potentiostat for low-power electrochemical applications

T. Tichter^{a,*}, M. Gernhard^b, P.C.K. Vesborg^a

^a Technical University of Denmark, Fysikvej 307, 2800 Kgs Lyngby, Denmark

^b Universität Bayreuth, Universitätsstr. 30, 95447 Bayreuth, Germany



ARTICLE INFO

Keywords:

Microcontroller based potentiostat for low power applications
Arduino Uno shield
Electrochemical analysis software
Cyclic voltammetry
Chronoamperometry

ABSTRACT

A potentiostatic circuit for low-power applications in the range of ± 3.3 V and ± 13.75 mA is developed. The device achieves a full-scale resolution of ≈ 1.6 mV and ≈ 1 μ A — sufficient for a wide range of electroanalytical experiments. For controlling the potentiostat a Python-based graphical user interface (GUI) is developed and implemented in our open-source electrochemistry software Polarographica. This enables electroanalytical experiments such as cyclic voltammetry (CV) and chronoamperometry (CA) in a live-graphing environment at an operational convenience similar to commercial devices, combined with a powerful tool for subsequent data analysis. The performance of our potentiostat is validated by the excellent agreement of CV and CA data acquired with five different in-house built devices and a commercial Gamry Reference 620. Finally, we provide a printed circuit board (PCB) design of our device as an Arduino shield that requires only a minimum of additional components. This powerful open-source tool is suitable for customized electrochemical experiments at material costs of less than 40 €.

1. Introduction

The instrumentation for controlling the bias of a working electrode with respect to a fixed reference potential in a three-electrode configuration was invented by Hickling in 1942 [1] and referred to as potentiostat. Nowadays, these devices are indispensable in any electrochemical laboratory. Distributed as blackboxes encapsulating the electronics, experimentalists do not have to worry about the internal circuit and the working principle of the machine. Instead, users are usually provided with a device which offers a multitude of specialized applications in a dynamic range of operating potentials and a neat software for interfacing and displaying the acquired data in a pre-processed form. However, in many cases only a very few of these built-in routines are frequently used. Consequently, commercial potentiostats are oftentimes severely overpowered – and hence overpriced – especially if only simple electroanalytical applications like stepping or sweeping potentials at moderate rates are needed. Moreover, if measurement routines differing from the build-in functions are required, a re-programming of the devices' internal software is a cumbersome task or even made impossible. Finally, since commercial potentiostats are designed for plug-and-play applications and not to be modified (for warranty reasons), the electrochemists' technical understanding of these devices becomes limited to common textbook-representations.

To mitigate the burden of costly equipment and to open the *potentiostatic blackbox*, various potentiostat projects have been reported in the past decade. An overview of the capabilities of the respective devices is given in Table 1.

Starting with the CheapStat project by Rowe [2] a potentiostat at costs of less than 80 € was introduced in 2011. Operating in a potential range of ± 0.99 V, the output capabilities of this device are, however, rather limited. These issues have been solved with the DStat – a potentiostat developed in 2015 by Dryden [3]. Employing an ATxmega256 microcontroller in combination with analog-to-digital converters (ADC) and digital-to-analog converters (DAC), the device achieves a remarkable accuracy in a voltage range of ± 1.5 V at a cost less than 120 €¹. Equipped with a Python-based graphical user interface (GUI) the DStat provides a convenient freeware solution and became thus a standard in the area of do-it-yourself (DIY) potentiostat solutions.

In 2016, Aremo [4] presented a DIY potentiostat based on the PIC18F452 microcontroller in combination with a R-2R resistor ladder as a 10-bit DAC. The device achieves a resolution of 5 mV and 50 μ A on a full scale of ± 2.5 V and ± 25 mA. Though the devices' performance is checked by investigating the Ni/Ni²⁺-redox reaction, a comparison to commercial potentiostats is not provided. Furthermore,

* Corresponding author.

E-mail address: tintic@gmx.de (T. Tichter).

¹ Original literature reports the values in US-dollar. These have been converted to Euro according to the mean exchange rate of the year 2022 (1.053 \$/€) to achieve a better comparison among different references

since subsequent data analysis for the strictly irreversible Ni-redox system is performed in terms of the reversible Randles-Ševčík equation the performance of the device remains unknown.

In the same year, an educational paper on an Arduino-based potentiostat at a cost of about 19 €¹ was published by Meloni [5]. The device uses an *RC*-low-pass filter as DAC for the 8-bit pulse-width modulation (PWM) of an Arduino Uno and a few amplifiers to create the triangular ramp required for measuring cyclic voltammetry. This introduces a lot of noise and achieves a full-scale resolution of only 20 mV — sufficient for educational, but not for analytical purposes. Furthermore, it is important to note that working and counter electrode are flipped in this design. Since data is sent through the serial interface of the Arduino and is meant to be received by a serial monitor, it can only be displayed subsequently to measurements.

Another potentiostatic circuit using the LMP91000 sensing chip and an Arduino Uno for communication with the PC was proposed in 2017 [6]. Reference measurements, comparing the device with a commercial Autolab PGSTAT show a rather poor agreement (i.e. presented CV traces deviate by more than 100 mV and possess several kinks when compared to the commercial device).

In 2018, an Arduino based potentiostat was proposed by Li [7]. Though still limited to the 8-bit PWM of the Arduino in combination with an *RC*-filter, the authors provide a graphical user interface written in proprietarily licensed LabVIEW which results in an improved operational convenience. Two additional publications from 2018 are presented in Refs. [8,9], where Ref. [8] is essentially a copy of the design by Meloni. Ref. [9] on the other hand uses a Raspberry Pi computer as replacement for the Arduino and equips the device with a touchpad for portable applications. By using external 12-bit DAC and ADC modules an operational range of ±4 V and ±20 mA with a resolution of 2.4 mV is achieved. Though not compared to commercial devices, the data presented in ref. [9] exhibits very little noise. This might essentially result from the authors effort in removing ripple from the voltage supply rails by including low-dropout voltage regulators in the circuit.

In 2019, the ABE-Stat — a wireless potentiostat based on the ESP8266 microcontroller — was developed by Jenkins et al. Their device utilizes a 16-bit DAC and a 24-bit ADC and is capable of performing CA, CV and fundamental electrochemical impedance spectroscopy (EIS) measurements. The performance of the potentiostat shows a very good agreement with data acquired with commercial devices. However, the circuit is already rather complex and with approximately 99 €¹ for material costs at least five times as expensive as the Arduino based devices.

In 2020, a six-channel potentiostat for monitoring the glucose concentration during fermentation processes was published in Ref. [10]. The device is based on an ATmega 2560 microcontroller in combination with a 16-bit DAC (AD5752) and a 16-bit ADC (AD7656). The performance is compared to a commercially available PalmSens3 potentiostat and shows a very good agreement for CV. Furthermore, the authors provide a LabVIEW based GUI for interfacing with the device. A second potentiostatic circuit, which was proposed in 2020, can be found in Ref. [11]. Aiming to minimize the size of the circuit to fit onto a micropipettor for on-site electrochemical characterizations, the authors utilize an Arduino Nano, a 12-bit DAC (MCP4921) and a 12-bit ADC (MCP3202). Controlling the device is realized via smartphone over bluetooth. Two additional potentiostat projects reported in the same year can be found in Refs. [12,13], where [12] is formally identical with the design of Meloni, apart from using a Node MCU ESP32 microcontroller instead of an Arduino Uno and Ref. [13], as a two electrode device, is not too practical.

In 2021, a series of home-built potentiostats have been published [14–20] among which, regarding the hardware, the MYSTAT project from Irving [18] is probably the most advanced DIY potentiostat to date. Using a PIC16F1459 microcontroller, a 20-bit DAC (DAC1220) and a 22-bit ADC (MCP3550-60) and implementing four current ranges,

the device covers remarkable ±200 mA at ±12 V, and is (regarding the operational range) comparable with commercial potentiostats. Furthermore, it can be operated as either a potentiostat or a galvanostat. In this context it is, however, worth to note that solely the Texas Instruments DAC1220 costs as much as the entire potentiostat of Ref. [5] and that the 15SPS conversion rate of the 22-bit ADC is very slow. The latter drawback becomes limiting for experiments using higher potential sweep rates. Consequently, the device might be modified by using an ADC with a lower resolution and a higher sampling speed (e.g. the ADS1115 or ADS1015).

Apart from the potentiostat/galvanostat function of the MYSTAT, the device presented by Matsubara [19] features the additional capability of measuring electrochemical impedance spectroscopy (EIS). At a cost of 410 €¹ this open source device can be thus a powerful addition to the laboratory. The device presented in Ref. [17] can be considered as an improved version of the design by Meloni [5]. Using an Arduino Mega in combination with an external 12-bit DAC (MCP4725) and an additional 12-bit ADC (ADS1015), the potentiostat avoids the drawbacks of combining the 8-bit PWM of the Arduino with an *RC* low-pass filter. Regarding the circuit, the operational ranges are limited to ±5 V and ±200 μA.

Recently, two different potentiostat projects have been presented. The ACEstat [21] is based on the ADuCM355-microchip, specifically designed for chemical sensing purposes. Implementing CA, CV, and EIS, the emphasis of this project is to unlock the capabilities of recent integrated circuit (IC) potentiostats such as the EMstat-Pico and to allow for miniaturization of potentiostat projects. The PassStat [22] is basically an assembly of four different open-source potentiostats for computer or smartphone controlled measurements. Implementing the Teensy 3.6 USB microcontroller or the Analog Discovery 2 USB oscilloscope, the devices' costs (and capabilities) range from 10 € to 300 €. Interfacing with the potentiostats is performed with either Android Studio, a combined Android/Python software or, in case of the USB oscilloscope solution, via Waveforms from Digilent.

1.1. Novelty of the recent work

Summarizing the aforementioned publications and consulting Table 1 it is seen that none of the projects provides an integration of the hardware with a software tool specifically designed for subsequent analysis of voltammetric data. Solving this demand is hence the emphasis of the present paper. Herein, we propose a potentiostat — the PolArStat — which is interfaced through the live-graphing, Python based, GUI of our open-source software Polarographica [23]. In this manner, a standalone tool for the acquisition, simulation, and fitting of voltammetric data is provided. The hardware builds upon the work of Meloni [5] and Farhan [17] and is designed as an open-source PCB shield for the Arduino Uno. The firmware for the PolArStat is written in C++ and contains pre-built functions for CV, CA and a calibration routine. Equipped with an external 12-bit DAC (MCP4725) and a 16-bit ADC (ADS1115), the PolArStat can operate at ±3.3 V and ±13.75 mA at a full-scale resolution of ≈1.6 mV and ≈1 μA. This results in an excellent agreement of electrochemical data acquired with PolArStat and a commercial potentiostat solution.

2. Circuit design

The potentiostatic circuit developed in this project is depicted in Fig. 1. It involves 8 operational amplifiers, 15 resistors, external integrated circuit (IC) DAC and ADC chips, a cell-switching Reed-relay, a protective zener diode and a cell on/off LED. The specifications and costs of these components are summarized in Table 2.

Apart from them, the circuit does only require an Arduino Uno and a symmetrical dual-rail power supply (which can be composed of two

Table 1

Overview on different DIY potentiostat projects of the last decade. It can be seen that none of the projects provides the potentiostat with a software for analysis of voltammetric data such as CV or CA.

E-range	I-range	bit-ADC/DAC	Cost	GUI	Ana.-softw.	Ref.
±0.99 V	±50 μ A	N/A	80 €	yes	no	[2]
±2.5 V	±0.5 mA	N/A	50 €	no	no	[24]
±0.5 V	±0.5 μ A	16/16	N/A	yes	no	[25]
±1.5 V	N/A	24/16	120 €	yes	no	[3]
±2.5 V	±25 mA	10/10	N/A	no	no	[4]
±2.5 V	±0.2 mA	10/8	30 €	no	no	[5]
±0.6 V	±60 μ A	N/A	N/A	no	no	[6]
±2.5 V	±10 mA	10/8	40 €	yes	no	[7]
±4 V	±20 mA	12/12	100 €	no	no	[9]
±1 V	±1 mA	10/8	N/A	no	no	[8]
±1.65 V	±10 mA	24/16	100 €	yes	no	[26]
±5 V	±50 mA	16/16	N/A	yes	no	[10]
±0.5 V	-50 to +30 μ A	10/8	60 €	yes	no	[12]
±1.65 V	±10 μ A	12/12	N/A	yes	no	[11]
±1.5 V	±15 μ A	16/12	55 €	yes	no	[13]
-1 to +2 V	±1 mA	12/8	N/A	yes	no	[14]
±1.5 V	±10 mA	16/12	50 €	yes	no	[15]
±4 V	±5 mA	16/12	70 €	yes	no	[16]
±5 V	±0.2 mA	12/12	N/A	yes	no	[17]
±12 V	±200 mA	22/20	220 €	yes	no	[18]
±12 V	±100 mA	14/x	375 €	yes	no	[19]
±2 V	±0.2 mA	10/8	30 €	no	no	[20]
±3.1 V	±3 mA	18/12	60 €	yes	no	[21]
±2.4 V	flex.	12/12	39-300 €	yes	no	[22]

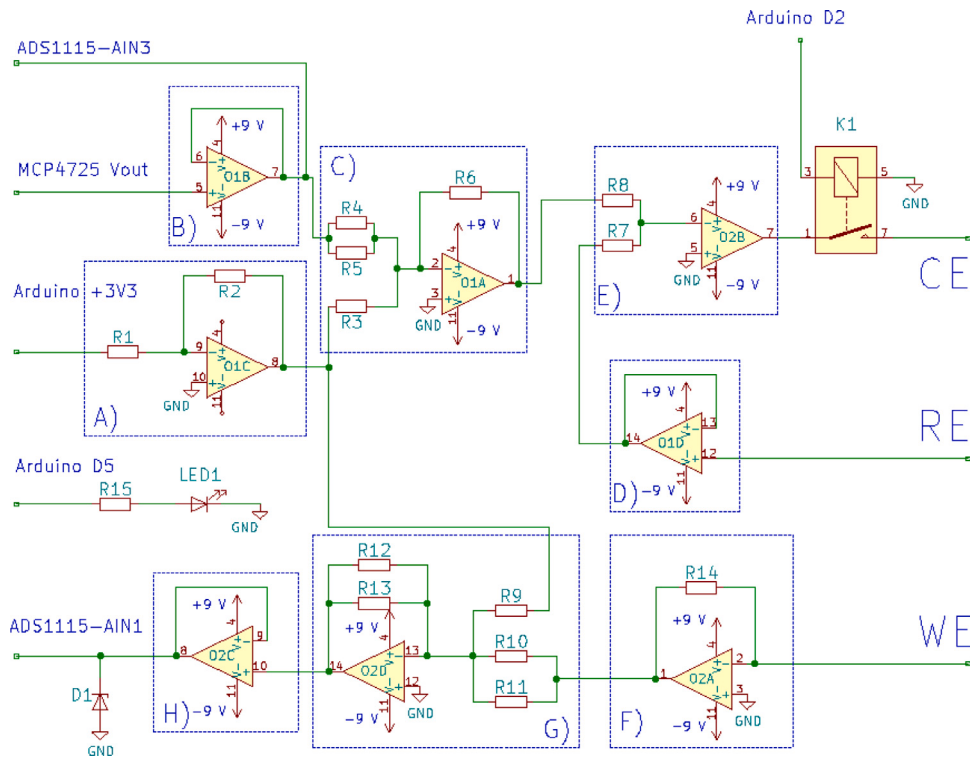


Fig. 1. Potentiostatic circuit developed in this work. All amplifiers are LM324N. Remaining components of the circuit are specified in Table 2.

9 V batteries² or salvaged from an old PC) to be a fully functional potentiostat. It should be noted that this particular potentiostatic circuit is reduced to essential components. Additional modifications for minimizing noise, increasing accuracy and protecting the electronics can be made, but will inevitable increase the costs and the complexity of the circuit. Nevertheless, they are discussed in the Section 6.

2.1. Building blocks of the circuit

The usual textbook representation of a potentiostat involves blocks (E), (D), and (F) of the circuit depicted in Fig. 1. For discussing this feedback system, as well as the remaining components, a fundamental understanding of operational amplifiers is required.

An operational amplifier is basically an active electronic component which is used to magnify minor potential differences between its two high impedance input terminals at a low impedance output. Generally, these devices output whatever voltage (within the capabilities of the power supply), required to compensate the potential difference

² Considering the battery-based solution with a capacity of about 260 mAh per 9 V block and the measured quiescent current of 3.5 mA, the power supply lasts for approximately 74 h.

Table 2

Pricing (October 2022) and specifications of the individual components of the PolArStat bought/ordered from (a) RS components, (b) amazon, (c) mouser electronics, (d) JLPCB.

Component	Label	Specification	Quant.xprice
Resistance (I)	R1–R6, R9–R13	1 kΩ±1%, (a)	12 × 0.05 €
Resistance (II)	R7, R8, R15	5.6 kΩ±1%, (a)	2 × 0.07 €
Resistance (III)	R14	120 Ω±1%, (a)	1 × 0.07 €
Amplifier	O1, O2	LM324N, (a)	2 × 0.36 €
DAC 12-bit	MCP4725	MCP4725, (b)	1 × 5.50 €
ADC 16-bit	ADS1115	ADS1115 (b)	1 × 3.10 €
Z-diode, 3.3 V	D1	1N4728A (a)	1 × 0.10 €
5V LED green	LED1	TLCPG5100 (c)	1 × 0.14 €
Reed-relay	K1	SIP-1A05 (b)	1 × 2.10 €
PCB shield	–	Custom, (d)	1 × 1.50 €
Arduino-Uno	–	— (b)	1 × 21.99 €
Alligator clips	–	— (b)	3 × 0.14 €
Total			36.38 €

between the input terminals. This features that operational amplifiers can be connected in certain configurations of which (I) buffering, (II) inflecting and (III) summing potentials are important for building a potentiostat.

Regarding Fig. 1 it can be seen that blocks (B), (D), and (H) are functionally identical. By tying back the output to the inverting input (negative) terminal, the operational amplifier will output the same potential w.r.t the circuit's ground as connected to the high-impedance path of the non-inverting (positive) input. Consequently, these amplifiers are used for an almost current free buffering of the input signals from (A) the digital to analog converter, (D) the reference electrode and (H) the signal obtained from block (G). Especially regarding block (D), this represents the high impedance path of the reference electrode required for a potentiostat to function.

Block (A) in Fig. 1 is configured as an inverting operational amplifier which is used to create a negative voltage rail, symmetrical to the positive reference voltage of 3.3 V. By connecting the non-inverting input of this amplifier to the circuits ground this amplifier will output whatever voltage required to drive the inverting input to zero (the concept of a virtual ground). By using a symmetrical voltage divider consisting of $R1 = R2 = 1 \text{ k}\Omega$, this can only be achieved, if the output potential equals the negative of the input potential — thus -3.3 V . By exploiting this configuration we (a) avoid the use of an additional linear voltage regulator like in the circuit proposed in ref [5], (b) provide a negative voltage rail which is always symmetrical to the positive reference voltage, and (c) do not leave any terminal of the two LM324N packages unused.

Block (F) in Fig. 1 is used as a current-to-voltage converter. By connecting its non-inverting input to the circuits ground, the lead of the working electrode will be kept at virtual ground. According to Ohms law, the potential at the output block (F) has to be adjusted to $E_{\text{out},F} = -I \cdot R14$ for shunting any current across $R14$. This potential is then fed into block (G) — a summing-inverting amplifier — being functionally identical with block (C).

The configuration of a summing-inverting amplifier is based on the same voltage-divider principle as was used in block (A). By grounding the non-inverting input terminal, the inverting input is kept at virtual ground. Using block (C) as example, this entails the current flowing through resistors $R3$, $R4$ and $R5$ towards the amplifier has to be shunted across resistor $R6$, since the inverting input has an ideally infinite input impedance. Noting that $R3 = R4 = R5 = R6 = 1 \text{ k}\Omega$ this results in

$$E_{\text{out},C} = -1 \text{ k}\Omega \cdot \left[\frac{E_{\text{out},B}}{500 \text{ }\Omega} + \frac{E_{\text{out},A}}{1 \text{ k}\Omega} \right] = -[2 E_{\text{out},B} + E_{\text{out},A}], \quad (1)$$

which allows for a weighted summation of the negative reference voltage and the inputs from Block (B) or Block (F), respectively.

Table 3

Input and output voltages of blocks (A), (B) and (C) of Fig. 1 depending on the bit-index (IDX) of the DAC.

In (A)	Out (A)	IDX-MCP4725	In (B)	Out (B)	Out (C)
3.3 V	-3.3 V	0	0 V	0 V	3.3 V
3.3 V	-3.3 V	2047	1.65 V	1.65 V	0 V
3.3 V	-3.3 V	4095	3.3 V	3.3 V	-3.3 V

Table 4

Input and output voltages of blocks (F), (G) and (H) of Fig. 1, as well as the bit-index of the ADS1115-ADC, depending on the current flowing across the CE-WE path.

$I_{\text{CE-WE}}$	Out (F)	Out (G)	Out (H)	IDX (ADS1115)
13.75 mA	-1.65 V	3.3 V	3.3 V	26400
0 mA	0 V	1.65 V	1.65 V	13200
-13.75 mA	1.65 V	0 V	0 V	0

2.2. Working principle of the potentiostatic circuit

The potentiostatic circuit uses a 3.3 V architecture, supplied by the respective reference voltage of the Arduino Uno. Consequently, the MCP4725, as a 12-bit DAC, can output 4096 different potential values at a stepsize of $3300 \text{ mV}/2^{12} = 0.81 \text{ mV}$. This variable input signal is buffered in block (B) and, together with the negative reference voltage generated in block (A), fed into the summing-inverting amplifier of block (C). The input potentials are monitored at the output of block (B) by connecting it to pin 3 of the ADS1115 ADC-chip. The outputs of block (C), depending on the voltage provided by the DAC, are displayed in Table 3. It can be seen that the full potential span is 6.6 V which corresponds to a full-scale writing resolution of about 1.6 mV.

Since $R7 = R8$, the output of block (C) is symmetrically summed with the buffered potential of the reference electrode in block (E). Note that this amplifier is not in an open loop configuration (if the cell switch $K1$ is conductive) — the feedback path is provided through the connection along the reference electrode and block (D). Since the inverting input of the amplifier in block (E) is held at virtual ground, this component will source or sink whatever current along the path between counter electrode and working electrode, to drive the potential at the reference electrode (which is buffered in block (D)) to be the negative of the input voltage. Since the working electrode is kept at virtual ground, this introduces the desired behavior, that the WE is always at the input potential w.r.t. the RE, whereas the CE imposes whatever current required to do so. This current is converted into a voltage in block (F) by shunting it across resistor $R14$. Since currents can be positive or negative (depending on the WE being the sink or source), these voltages can be either positive or negative. To generate positive potentials only, the output of block (F) is passed through the summing-inverting amplifier in block (G). Considering that $R14 = 120 \Omega$, this gives the current ranges and resolutions as shown in Table 4.

Regarding Table 4, the maximum absolute current is 13.75 mA. This is a result of using $R14 = 120 \Omega$ in the current to voltage converter of block F in combination with a 3.3 V zener diode (D1) for protection of the circuit. In principle, the LM324N could source and sink a continuous current up to $\pm 20 \text{ mA}$. However, at absolute currents larger than 13.75 mA, D1 will partially shunt the output current and clipping of the measured signal will occur. The bit-indices given in Table 4 result from the fact that the ADS1115 (as a 16-bit ADC) achieves an effective 15-bit resolution (so $2^{15} = 32768$ points) in single-ended mode. Setting its internal programmable gain amplifier (PGA) to the range of 4.096 V (closest to the 3.3 V architecture used in this work) 26400 indices can be used effectively. Hence, a resolution of 26400 discrete points along the range of $\pm 13.75 \text{ mA}$ is achieved, which corresponds to a resolution of $1.04 \mu\text{A}$ and is sufficient for a multitude of experimentally relevant scenarios.

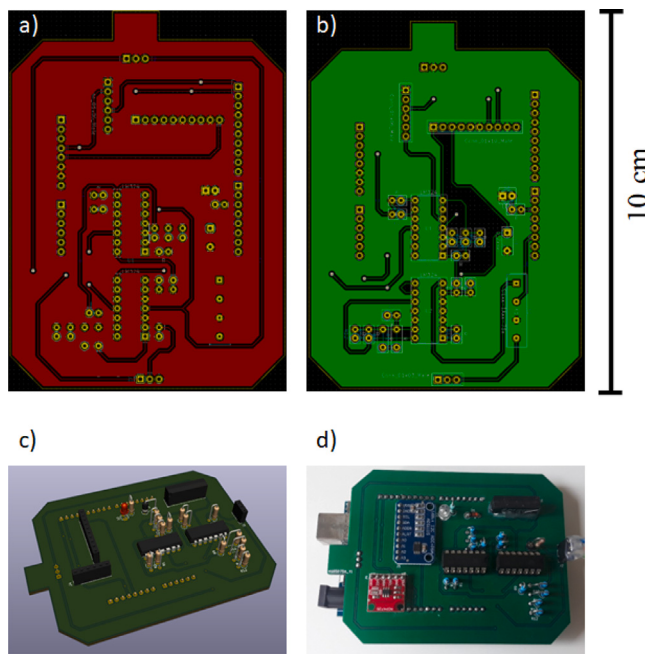


Fig. 2. Panel (a) frontside, (b) backside and (c) CAD model of the PCB shield for the potentiostatic circuit developed in this work. Panel (d) photograph of the assembled device.

3. Hardware design

Designing the potentiostat as a printed circuit board (PCB) fitting an Arduino UNO R3 as a shield was done by using the software tool KiCAD. Fig. 2 depicts the (a) frontside, (b) backside, (c) CAD model, and (d) photograph of the assembled device. Respective Gerber-files for ordering the PCB-shield from an external manufacturer can be found in the supporting information or at GitHub along with our open-source software Polarographica. Provided the components listed in Table 2 are accessible, assembling the potentiostat takes approximately 40 min. A detailed guide on how to assemble the PolArStat can be found in the supporting information.

4. Software development

The software required for controlling the potentiostat is divided into (I) a firmware script which is uploaded to the microcontroller for receiving commands from and sending data to the computer and (II) a software script which is running on the computer for sending commands and receiving data.

The firmware for the device is written in C++ using the Arduino IDE. It can be downloaded as open-source code from our GitHub project Polarographica and is attached as supplementary file as well.

The software for controlling the potentiostat is a Python script with a graphical user interface. The communication is facilitated over USB connection using serial interfacing accessible through the pySerial module. Implemented in our open-source electroanalytical software Polarographica users are provided with a powerful platform for conducting voltammetric experiments at an operational convenience similar to commercial potentiostats. As an example, Fig. 3 shows the cyclic-voltammetry function in our software.

Subsequently to choosing a serial port (in case multiple serial ports are connected to the computer) and starting the serial connection, CV can be measured. A similarly straightforward GUI is accessible for chronoamperometry as well as for a calibration of the device.

5. Experimental benchmarking

Validating the experimental performance of the potentiostat is performed in a two-step procedure. First, a 1 k Ω precision resistor ($\pm 1\%$) is used as a dummy in a linear-sweep-voltammetry (LSV) experiment spanning the full scale of potentials (i.e. ± 3.3 V). For this purpose, the device was set up in a two electrode configuration (i.e. in the connection RE/CE—WE). The result of this checkup is depicted in Fig. 4.

In another experiment, the performance of the PolArStat is thoroughly validated in a true electrochemical system by measuring cyclic voltammetry and chronoamperometry for five different devices and by comparing the results with a commercial Gamry Ref. [620]. As reference system, the electrochemical redox reaction of ferro/ferricyanide was studied at a 7 mm glassy carbon disc electrode. Electrolyte solutions were 1 M NaCl (Sigma Aldrich, BioXtra > 99.5%) containing 50 mM analytical grade K₄[Fe(CN)₆] (Merck). During the experiments, an Ag/AgCl electrode (Sigma Aldrich, Z113085, sat. NaCl) was used as reference (RE) and a platinum wire as counter electrode. Before each individual measurement, the working electrode was polished with alumina paste (MicroPolish, 0.3 μ m, Buehler) and thoroughly rinsed with ultrapure water (Millipore, 18.2 M Ω cm). Fig. 5 shows (a) 30 chronoamperometry measurements and (b) 30 cyclic voltammetry measurements (five for each PolArStat (gray traces) and five for the Gamry Ref. [620] (red traces)) to the conditions given in the caption. It can be seen that an excellent agreement between the acquired data is achieved.

To investigate the performance of our device at different potential sweep-rates, a Randles-Ševčík experiment has been conducted for five different PolArStat and the commercial Gamry Ref. [620]. In this experiment, only one CV has been acquired per device and sweep-rate. The data is shown in Fig. 6, where experimental parameters are given in the caption. It can be seen that also at larger potential sweep rates an excellent agreement of the data acquired with the PolArStat and the commercial device is achieved.

5.1. CV-analysis with Polarographica

Subsequently to performing voltammetric experiments with the PolArStat, the acquired data can be analyzed directly in the environment of Polarographica [23] which is one of the major advantages of this project. Using the CV-fitting function³ for planar semi-infinite diffusion on one of the CV-datasets in Fig. 5, a good agreement between simulated and experimentally acquired data is achieved (cf. Fig. 7).

The estimated diffusion coefficient for ferrocyanide of

$D = 7.2 \text{ cm}^2/\text{s}$ is also in line with the literature value [28] of $D = 7.26 \text{ cm}^2/\text{s}$ which underlines that the PolArStat performs accurately at a quantitative scale. However – and even more important – it demonstrates that the combination of the PolArStat and Polarographica provides a powerful open-source solution for performing electroanalytical experiments and analyzing voltammetric data.

6. Additional modifications

This section suggests a few modifications of the PolArStat which could be done for increasing the robustness of the device and for minimizing noise. However, these are optional, will contribute to the cost and complexity of the circuit and potentially require a modification of the PCB. Moreover, they would need to be validated experimentally by the user.

Reference buffering: LM324 has an input bias-current of about 100 nA. This can become problematic in block (D), where it is used for buffering the potential of the reference electrode. Using an operational amplifier with a larger input impedance could be beneficial in this

³ For details on the CV-fitting process with Polarographica see [27]

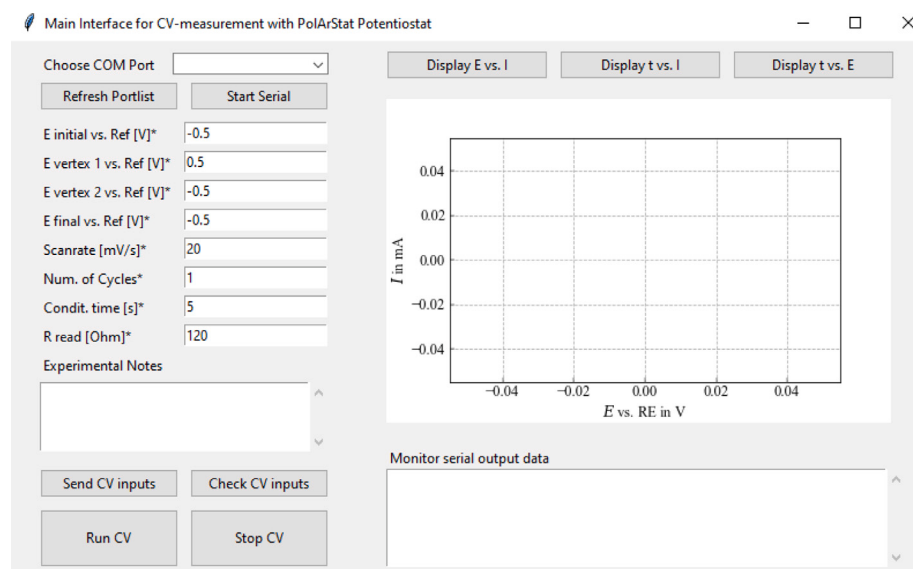


Fig. 3. Graphical user interface (GUI) for measuring cyclic voltammetry with the PolArStat.

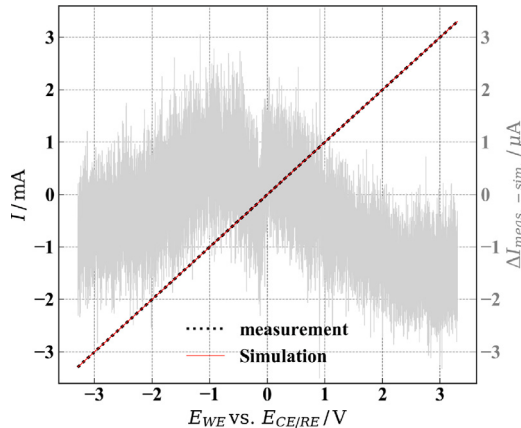


Fig. 4. Linear-sweep-voltammetry of a $1\text{ k}\Omega$ precision resistor ($\pm 1\%$) acquired with a PolArStat (black dotted line) as well as a simulation of an Ohmic resistor of exactly $1\text{ k}\Omega$ (red line). The gray curve, scaling on the secondary ordinate, depicts the residuals between measurement and simulation. It can be seen that the absolute error is less than $3\text{ }\mu\text{A}$ at any potential. In a linear fitting a resistance of $999.8\text{ }\Omega$ was found, which is in the range of error tolerance of the precision resistor.

case as this will reduce a potential drift of the reference electrode over time. Despite the fact that none of our experimental benchmarking studies revealed a drift of the reference potential, we want to draw the readers attention to the fact that this can potentially cause problems and suggest a possible solution. One option would be the use of TL074 instead of LM324. This amplifier has the same pinout as the LM324 with an input offset current of only 100 pA . Likewise, it can be used without changing the PCB. Since both, LM324 and TL074 are quad-operational amplifiers, using TL074 in block (D) will also use TL074 in blocks (A), (B), (C) which is, however, no problem. Nevertheless, the reader should be aware of the fact that TL074 is about six times as expensive as LM324.

Noise minimization: Additional components for filtering noise can be added to the circuit. These will, however, require a modification of the PCB in most cases. Changes may involve:

- In block (A), which creates the negative reference voltage, R_1 and R_2 can be changed to $10\text{ k}\Omega$ and an additional pull-down capacitor of $10\text{ }\mu\text{F}$ can be added between them. This would create

an RC-low-pass filter with a cutoff frequency of 1.59 Hz and attenuate potential noise created by the power supply of the Arduino-Uno board. While changing R_1 and R_2 will not require a modification of the PCB, including a capacitor will.

- In the case that two 9 V batteries are used as DC power supply, the modification of this bullet point is obsolete. However, in case of an external – potentially noisy – DC power source, it can be advantageous to stabilize the supply voltage of the operational amplifiers. This can be done by adding capacitors of $0.1\text{ }\mu\text{F}$ across the terminals. This particular modification will, however, require a modification of the PCB.
- Operational amplifiers can also be a source of noise. Replacing LM324 with TL074 (see above) will reduce the noise density from 40 nV/Hz to 18 nV/Hz . This modification will not require a change of the PCB.

Protection of equipment: Relay K_1 , which is essential for decoupling the counter electrode in non-active mode, may cause two problems.

- It could harm the digital pin D2 of the Arduino-Uno board over time, as any closing/opening event creates a kickback-voltage in its coils. Such a problem was, however, never observed by us. Nevertheless, a possible solution for avoiding kickback-voltage spikes would be the addition of a protection diode between the Arduino pin D2 and the ground. A respective modification will, however, require a modification of the PCB.
- As long as K_1 is left open, amplifier O2B in block (E) will output its rail-voltage of $\pm 9\text{ V}$. As soon as K_1 closes (so if a measurement starts), O2B will require a short time to settle to the desired voltage which creates a voltage spike between working electrode and counter electrode. Even if this artifact is not seen in the measurements since the ADS1115 is too slow for resolving it, large voltage spikes could potentially harm the working electrode. However, it is worth to note that in our experiments such behavior was not observed. Nevertheless, this effect could be reduced by replacing LM324 by an operational amplifier with a higher slew-rate such that the voltage settles faster. Again, TL074 might be a choice, as its slew rate is approximately 26-times larger than for LM324.

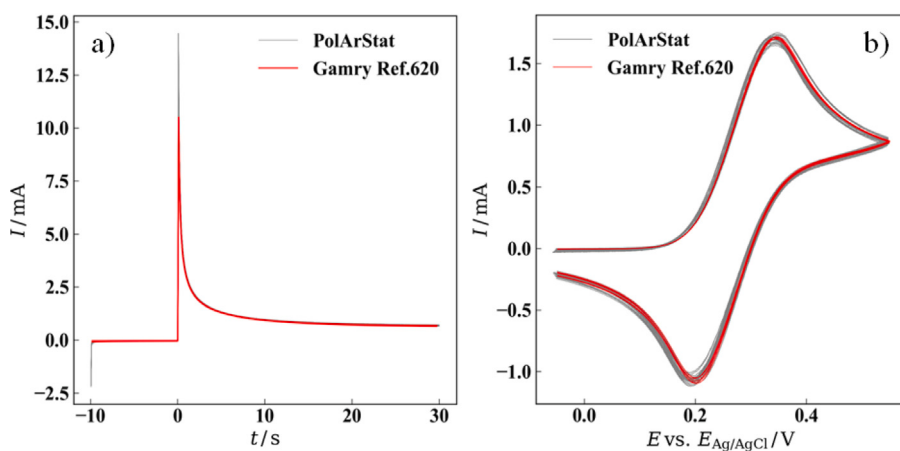


Fig. 5. Panel (a): Chronoamperometry measurements stepping the potential from -0.05 V vs. RE to 0.55 V vs. RE after a conditioning period of 10 s . Panel (b) Cyclic voltammetry measurements at 20 mV/s between -0.05 V vs. RE to 0.55 V vs. RE after a conditioning at -0.05 V vs. RE for 5 s . Experiments were conducted in 1 M NaCl , containing 50 mM ferrocyanide as analyte. Electrodes were WE: mirror-polished glassy carbon, $d = 7 \text{ mm}$, CE: Pt-wire, RE: Ag/AgCl sat. NaCl . The initial scanning direction was positive.

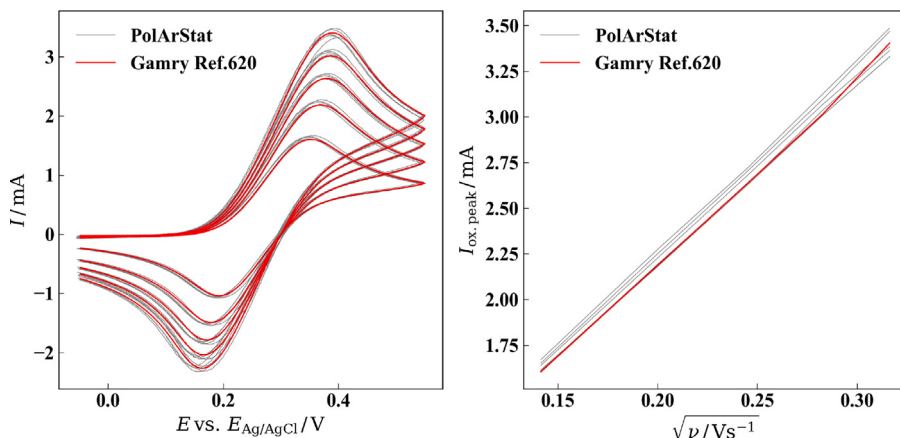


Fig. 6. Randles-Ševčík experiment at sweep-rates of 100 , 80 , 60 , 40 and 20 mV/s for five PolArStat (gray) and one Gamry Ref. [620] potentiostat (red). Plotting the peak current w.r.t. the potential sweep rate yields straight lines in all cases. Experiments were conducted in the same system as for Fig. 5.

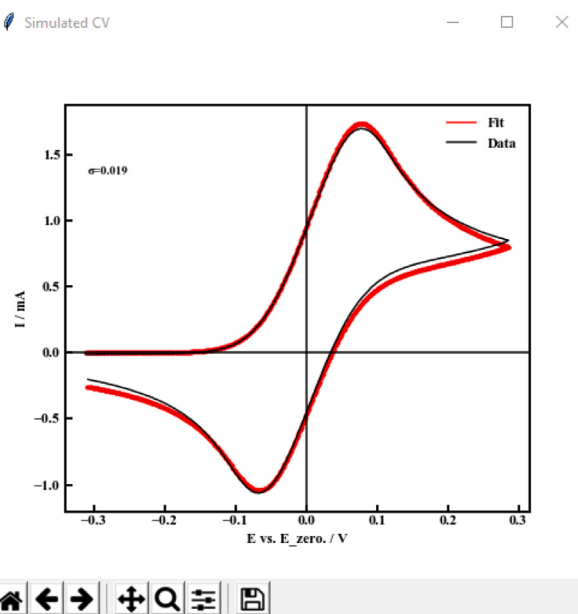


Fig. 7. CV data acquired for the electrochemical oxidation of ferrocyanide with a PolArStat (black trace) fitted with the planar semi-infinite diffusion model in Polarographica (red trace).

7. Summary and conclusions

In this work a potentiostatic circuit was developed in the form of a printed circuit board fitting on top of a classical Arduino UNO in the form of a shield. Using only a very few standard operational amplifiers, resistors, an external digital-to-analog and analog-to-digital converter the material costs of the project are less than 40 € (of which the majority cost is the Arduino). An open-source firmware for receiving and sending data from and to the computer, for performing cyclic voltammetry (CV) and chronoamperometry (CA) or for calibrating the device is provided as a classical Arduino sketch which can be readily uploaded to the microcontroller, using the Arduino integrated development environment (IDE). A graphical user interface with a live-updating console is provided as a Python script. This allows the instrument to perform CV and CA measurements in a manner similar to commercially available potentiostats. Finally, this function is implemented in our open-source electroanalytical tool Polarographica which provides users with a standalone software for measuring, simulating and evaluating voltammetric experiments without the need of commercial software or hardware.

CRediT authorship contribution statement

T. Tichter: Conceptualization, Methodology, Software, Hardware design, Validation, Visualization, Writing – original draft, Writing –

review & editing. **M. Gernhard:** Formal analysis, Methodology, Software, Validation, Writing – review & editing. **P.C.K. Vesborg:** Supervision, Writing – original draft, Writing – review & editing, Funding acquisition.

Declaration of competing interest

The authors declare that they have no known competing financial interests or personal relationships that could have appeared to influence the work reported in this paper.

Data availability

Data will be made available on request.

Acknowledgment

This work was supported by a research grant (DFF-0217-00333) from Danmarks Frie Forskningsfond.

Appendix A. Supplementary data

Supplementary material related to this article can be found online at <https://doi.org/10.1016/j.electacta.2023.143119>.

References

- [1] A. Hickling, Studies in electrode polarisation. Part IV.—The automatic control of the potential of a working electrode, *Trans. Faraday Soc.* 38 (1942) 27–33, <http://dx.doi.org/10.1039/TF9423800027>.
- [2] A.A. Rowe, A.J. Bonham, R.J. White, M.P. Zimmer, R.J. Yadgar, T.M. Hobza, J.W. Honea, I. Ben-Yaacov, K.W. Plaxco, CheapStat: An open-source, “do-it-yourself” potentiostat for analytical and educational applications, *PLoS One* 6 (2011) 1–7, <http://dx.doi.org/10.1371/journal.pone.0023783>.
- [3] A.R. Dryden, DStat: A versatile, open-source potentiostat for electroanalysis and integration, *PLoS One* 10 (2015) 1–17, <http://dx.doi.org/10.1371/journal.pone.0140349>.
- [4] B. Aremo, A.M. Oyebamiji, I.B. Obioho, O.A. Adeboye, A simplified microcontroller based potentiostat for low-resource applications, *Open J. Metal* 5 (2016) 37–46, <http://dx.doi.org/10.4236/ojmetal.2015.54005>.
- [5] G.N. Meloni, Building a microcontroller based potentiostat: A inexpensive and versatile platform for teaching electrochemistry and instruments, *J. Chem. Educ.* 93 (2016) 1320–1322, <http://dx.doi.org/10.1021/acs.jchemed.5b00961>.
- [6] P. Bezuidenhout, S. Smith, K. Land, T.-H. Joubert, A low-cost potentiostat for point-of-need diagnostics, in: 2017 IEEE AFRICON, 2017, pp. 83–87, <http://dx.doi.org/10.1109/AFRCON.2017.8095460>.
- [7] Y.C. Li, E.L. Melenbrink, G.J. Cordonier, C. Boggs, A. Khan, M.K. Isaac, L.K. Nkhonjera, D. Bahati, S.J. Billinge, S.M. Haile, R.A. Kreuter, R.M. Crable, T.E. Mallouk, An easily fabricated low-cost potentiostat coupled with user-friendly software for introducing students to electrochemical reactions and electroanalytical techniques, *J. Chem. Educ.* (2018) 1658–1661, <http://dx.doi.org/10.1021/acs.jchemed.8b00340>.
- [8] S.N.H. Umar, E.A. Bakar, N.M. Kamaruddin, N. Uchiyama, A Low Cost Potentiostat Device For Monitoring Aqueous Solution, in: MATEC Web Conf., Vol. 217, 2018, p. 04001, <http://dx.doi.org/10.1051/matecconf/201821704001>.
- [9] T. Nagata, K. Suzuki, Building a low-cost standalone electrochemical instrument based on a credit card-sized computer, *Anal. Sci.* 34 (2018) 1213–1216, <http://dx.doi.org/10.2116/analsci.18A002>.
- [10] S. Abdullah, M. Serpelloni, E. Sardini, Design of multichannel potentiostat for remote and longtime monitoring of glucose concentration during yeast fermentation, *Rev. Sci. Instrum.* 91 (2020) 054104, <http://dx.doi.org/10.1063/1.5137789>.
- [11] J.T. Barragan, L.T. Kubota, Minipotentiostat controlled by smartphone on a micropipette: A versatile, portable, agile and accurate tool for electroanalysis, *Electrochim. Acta* 341 (2020) 136048, <http://dx.doi.org/10.1016/j.electacta.2020.136048>.
- [12] M.A.M. Azmi, M.S. Zulkornain, F. Makmon, Development of handheld electronic reader based potentiostat for electrochemical analysis, *AIP Conf. Proc.* 2291 (2020) 020015, <http://dx.doi.org/10.1063/5.0027895>.
- [13] M.W. Glasscott, M.D. Verber, J.R. Hall, A.D. Pendergast, C.J. McKinney, J.E. Dick, SweepStat: A build-it-yourself, two-electrode potentiostat for macroelectrode and ultramicroelectrode studies, *J. Chem. Educ.* 97 (2020) 265–270, <http://dx.doi.org/10.1021/acs.jchemed.9b00893>.
- [14] F. Alam, M.M. Hasan, M.R. Siddiquee, S. Forouzanfar, A.H. Jalal, N. Pala, Miniaturized, wireless multi-channel potentiostat platform for wearable sensing and monitoring applications, in: Smart Biomedical and Physiological Sensor Technology XVIII, Vol. 11757, 2021, p. 117570H, <http://dx.doi.org/10.1117/12.2587955>.
- [15] A.R. Baranwal, S. Dudala, P. Rewatkar, J.M. Mohan, M. Salve, S. Goel, Development of completely automated poly potential portable potentiostat, *J. Solid State Sci. Technol.* 10 (2021) 027001, <http://dx.doi.org/10.1149/2162-8777/abdc15>.
- [16] A. Das, S. Bose, N. Mandal, B. Pramanick, C. RoyChaudhuri, HOME-stat: a handheld potentiostat with open-access mobile-interface and extended measurement ranges, *Proc. Indian Natl. Sci. Acad.* 87 (2021) 84–93, <http://dx.doi.org/10.1007/s43538-021-00008-7>.
- [17] I.M. Farhan, M.N. Aldy, J. Nabillah, F. Adriyanto, Design of microcontroller-based potentiostat for determination of ethanol integrated with smartphone through Internet of Things, *IOP Conf. Ser. Mater. Sci. Eng.* 1096 (2021) 012073, <http://dx.doi.org/10.1088/1757-899x/1096/1/012073>.
- [18] P. Irving, R. Cecil, M.Z. Yates, MYSTAT: A compact potentiostat/galvanostat for general electrochemistry measurements, *HardwareX* 9 (2021) e00163, <http://dx.doi.org/10.1016/j.hbx.2020.e00163>.
- [19] Y. Matsubara, A small yet complete framework for a potentiostat, galvanostat, and electrochemical impedance spectrometer, *J. Chem. Educ.* 98 (2021) 3362–3370, <http://dx.doi.org/10.1021/acs.jchemed.1c00228>.
- [20] D.V. Thomaz, U.A. Contardi, M. Morikawa, P.A. dos Santos, Development of an affordable, portable and reliable voltammetric platform for general purpose electroanalysis, *Microchem. J.* 170 (2021) 106756, <http://dx.doi.org/10.1016/j.microc.2021.106756>.
- [21] E.W. Brown, M.W. Glasscott, K. Conley, J. Barr, J.D. Ray, L.C. Moores, A. Netchaev, Acestat: A DIY guide to unlocking the potential of integrated circuit potentiostats for open-source electrochemical analysis, *Anal. Chem.* 94 (2022) 4906–4912, <http://dx.doi.org/10.1021/acs.analchem.1c04226>.
- [22] M. Caux, A. Achit, K. Var, G. Boitel-Aullen, D. Rose, A. Aubouy, S. Argentieri, R. Campagnolo, E. Maisonneuve, PassStat, a simple but fast, precise and versatile open source potentiostat, *HardwareX* 11 (2022) e00290, <http://dx.doi.org/10.1016/j.hbx.2022.e00290>.
- [23] T. Tichter, J. Schneider, Polarographica program, 2019, URL http://github.com/Polarographica/Polarographica_program.
- [24] J.R. Mott, P.J. Munson, R.A. Kreuter, B.S. Chohan, D.G. Sykes, CheapStat: An open-source, “do-it-yourself” potentiostat for analytical and educational applications, *J. Chem. Educ.* 91 (2014) 1028–1036, <http://dx.doi.org/10.1021/ed4004518>.
- [25] K. Kellner, T. Posniecek, J. Ettenauer, K. Zuser, M. Brandl, A new, low-cost potentiostat for environmental measurements with an easy-to-use PC interface, *Procedia Eng.* 120 (2015) 956–960, <http://dx.doi.org/10.1016/j.proeng.2015.08.820>.
- [26] D.M. Jenkins, B.E. Lee, S. Jun, J. Reyes-De-Corcuera, E.S. McLamore, ABESTat, a fully open-source and versatile wireless potentiostat project including electrochemical impedance spectroscopy, *J. Electrochem. Soc.* 166 (2019) B3056, <http://dx.doi.org/10.1149/2.0061909jes>.
- [27] T. Tichter, J. Schneider, D. Andrae, M. Gebhard, C. Roth, Universal algorithm for simulating and evaluating cyclic voltammetry at macroporous electrodes by considering random arrays of microelectrodes, *ChemPhysChem* 21 (2019) 428–441, <http://dx.doi.org/10.1002/cphc.201901113>.
- [28] S.J. Konopka, B. McDuffie, Diffusion coefficients of ferri- and ferrocyanide ions in aqueous media, using twin-electrode thin-layer electrochemistry, *Anal. Chem.* 42 (1970) 1741–1746, <http://dx.doi.org/10.1021/ac50160a042>.